UPWIND FINITE DIFFERENCE SOLUTION OF BOLTZMANN EQUATION APPLIED TO ELECTRON TRANSPORT IN SEMICONDUCTOR DEVICES

By

Emad Fatemi

and

Faroukh Odeh

IMA Preprint Series # 980

May 1992

Upwind Finite Difference Solution of Boltzmann Equation Applied to Electron Transport in Semiconductor Devices

Emad Fatemi [1] and Faroukh Odeh [2]

Institute for Mathematics and Its Applications, Minneapolis, MN 55455

IBM T.J. Watson Research Center, Yorktown Heights, NY 10598

Subject Classification: 65M06, 82C70, 82C80

Key Words: Boltzmann Equation , Upwind Schemes, Semiconductor Devices

[1]This research was supported in part by the Institute for Mathematics and its Applications with funds provided by the National Science Foundation

[2]Regrettably Faroukh is no longer with us. His sudden death was a big loss for his friends and colleagues. He will be remembered for his gentle and generous soul.

Running Head: Finite Difference Solution of Boltzmann

Proofs to be sent to:

Emad Fatemi

Institute for Mathematics and its Applications

University of Minnesota

514 Vincent Hall

206 Church st. S.E.

Minneapolis, MN 55455

Abstract

In this paper we present a new numerical method for solving Boltzmann transport equation describing charge transport in semiconductor devices. The Boltzmann equation is reduced to two dimensions in velocity space by assumption of density being invariant under rotations around z axis. We developed a finite difference discretization of Boltzmann Equation in one spatial dimension and two dimensional velocity space, coupled to the Poisson equation. First three moments of BTE coupled to the Poisson equation is known as the Hydrodynamic model. A comparison of the numerical results from this method and the Hydrodynamic model is given. Also a numerical investigation is done with respect to the heat conduction, viscosity, and momentum relaxation terms in the Hydrodynamic model.

1 Introduction

Charge transport in semiconductor devices can be modeled semi-classically via Boltzmann transport equation. The Boltzmann equation is an Integro-Differential equation in seven dimensions, three in space, three in velocity space, and one in time. At present, full discretization of BTE is out of range of existing computers. A very popular method for solving BTE is the Monte Carlo method. For a comprehensive and tutorial review of this method we refer the reader to the article by C. Jacoboni and L. Reggiani[9]. Because Monte Carlo method relies on random sampling the results are often noisy. Another approach to solving BTE is particle method. In this approach the collision integrals are calculated deterministically [12]. In this paper we develop an upwind finite difference approximation of the differential terms. The collision integrals were calculated numerically. This method is closely related to methods developed for solving kinetic equations for neutron transport [10].

By taking the first three moments of the BTE one obtains conservation laws for mass, momentum, and energy. This will result in a system of five equations with fourteen variables in three-dimensional space. In order to close the system one needs to make certain assumptions. With assumption of pressure tensor to be scalar and heat flux to be defined by Fourier Law,[3] , one obtains Euler equations of gas dynamics with source terms and heat conduction. Scattering terms are replaced with relaxation time approximation. This system coupled to the Poisson equation is known as the "Hydrodynamic Model" in semiconductor modeling[1] .

A simpler and more widely used model is Drift-Diffusion. One can interpret it as conservation of mass and a simplified version of conservation of momentum equation with assumption of constant temperature and small Mach number. Drift-Diffusion model loses its accuracy as the size of the device becomes less than one micron.

In this paper we solve the BTE numerically. Once the distribution function is found we can take moments and recover various terms in the Hydrodynamic model. The Hydrodynamic model was solved using sixth order ENO shock capturing algorithms [3], [14]. Using

numerical results from BTE one can check the accuracy of various approximations in the Hydrodynamic model.

2 Boltzmann Equation

Let $f(\mathbf{x},\mathbf{u},t)$ be the probability density function of electrons, where $\mathbf{x} = (x,y,z)$ is the space variable and $\mathbf{u} = (u,v,w)$ is the velocity variable. Then the dynamics of electrons can be modeled by:

$$f_t + \mathbf{u}\nabla_{\mathbf{x}} f + \mathbf{F}\nabla_{\mathbf{u}} f = \int s(\mathbf{u}',\mathbf{u}) f(\mathbf{u}') d\mathbf{u}' - \int s(\mathbf{u},\mathbf{u}') f(\mathbf{u}) d\mathbf{u}', \tag{1}$$

$$\nabla.(\epsilon\nabla\phi) = e(-N_D + n), \tag{2}$$

$$(F_x, F_y, F_z) = \mathbf{F} = \frac{-e}{m}\mathbf{E} = \frac{e}{m}\nabla\phi.$$

$s(\mathbf{u},\mathbf{u}')$ is the scattering operator, ϕ is the electric potential, $\mathbf{E}$ is the electric field, N_D is the density of donors, e is charge of an electron, ϵ is the permittivity in the crystal, and $n = \int f(\mathbf{u})d\mathbf{u}$ is the density of electrons .

We scale the equations in the following fashion:

$$\bar{t}\tau_p = t, \quad \bar{x}L = x, \quad \bar{\mathbf{u}}U = \mathbf{u}, \quad \frac{\bar{S}}{\tau_p} = S, \quad \bar{\phi}\frac{mEL}{e} = \phi, \quad \bar{n}N = n.$$

We suppress the bar notation for the scaled quantities and get:

$$f_t + (\frac{U\tau_t}{L})\mathbf{u}\nabla_{\mathbf{x}} f + (\frac{E\tau_t}{U})\nabla\phi.\nabla_{\mathbf{u}} f = (\frac{\tau_t}{\tau_p})(\int s(\mathbf{u}',\mathbf{u}) f(\mathbf{u}') d\mathbf{u}' - \int s(\mathbf{u},\mathbf{u}') f(\mathbf{u}) d\mathbf{u}'), \tag{3}$$

$$\nabla.(\nabla\phi) = (\frac{e^2 LN}{\epsilon mE})(-N_D + n). \tag{4}$$

This leaves us four non-dimensional parameters:

$$\frac{U\tau_t}{L}, \qquad \frac{E\tau_t}{U}, \qquad \frac{\tau_t}{\tau_p}, \qquad \frac{e^2 LN}{\epsilon mE}.$$

If we let $\tau_t = L/U$, then for the considered problem we have:

$$\frac{U\tau_t}{L} = 1, \quad \frac{E\tau_t}{U} \approx 0.675, \quad \frac{\tau_t}{\tau_p} \approx 5 \sim 50, \quad \text{and} \quad \frac{e^2 LN}{\epsilon mE} \approx 150.$$

We identify the ratio $Kn = \frac{\tau_p}{\tau_t} = \frac{\tau_p U}{L}$ as the Knudsen number of the flow.

From the Boltzmann equation one can obtain conservation laws. We use the notation

$$< \psi(\mathbf{u}), f >= \int_{-\infty}^{+\infty} \int_{-\infty}^{+\infty} \int_{-\infty}^{+\infty} \psi(\mathbf{u}) f(\mathbf{u}) d\mathbf{u}$$

$$< \psi, f >_t + \nabla_{\mathbf{x}} < \mathbf{u}\psi, f >= \mathbf{F} < \nabla_{\mathbf{u}}\psi, f > + < \psi, S > \tag{5}$$

By taking $\psi = m, m\mathbf{u}, \frac{1}{2}m\mathbf{u}^2$ one recovers the Euler Equations of gas dynamics. These equations have been proposed by Bløtekjær [2] and have been studied numerically by [7], [13], [6], [3], [4]. Viscosity solutions of this system has been studied by [5]. In the Numerical calculations done in [3] non-physical velocity spikes were observed as electrons cross the channel to the drain. In this paper we try to resolve this issue. In particular we are interested in assessing the effect of approximations for heat conduction, viscosity, and momentum relaxation terms. Define $\mathbf{v}$ to be the average velocity, $\mathbf{v} = \frac{<\mathbf{u}, f>}{<1, f>}$. Then:

$$\frac{1}{2}m < (\mathbf{u} - \mathbf{v})^3, f >\approx \kappa n \nabla T,$$

$$\frac{1}{2}m < (\mathbf{u} - \mathbf{v})^2, f >= \begin{pmatrix} nT_{11} & nT_{12} & nT_{13} \\ nT_{21} & nT_{22} & nT_{23} \\ nT_{31} & nT_{32} & nT_{33} \end{pmatrix} \approx$$

$$\begin{pmatrix} nT & 0 & 0 \\ 0 & nT & 0 \\ 0 & 0 & nT \end{pmatrix} - \nu \begin{pmatrix} \frac{4}{3}u_x - \frac{2}{3}v_y - \frac{2}{3}w_z & u_y + v_x & w_x + u_z \\ u_y + v_x & \frac{4}{3}v_y - \frac{2}{3}u_x - \frac{2}{3}w_z & w_y + v_z \\ u_z + w_x & v_z + w_y & \frac{4}{3}w_z - \frac{2}{3}u_x - \frac{2}{3}v_y \end{pmatrix},$$

where temperature is defined as $T = \frac{T_{11}+T_{22}+T_{33}}{3}$ and $\nu = \tau_p nT$ is the coefficient of viscosity.

$$< \mathbf{u}S, f >\approx \frac{- < \mathbf{u}, f >}{\tau_p},$$

where τ_p is the momentum relaxation time. We use the results from BTE code to verify the models for κ and τ_p; $\kappa = \frac{3\mu_0 k_b^2 T_0}{2e}$, and $\tau_p = \frac{m\mu_0 T}{eT}$.

3 Transformation to Polar Coordinates

We consider a case where electric field is in the z axis direction. That implies that the problem is invariant under rotations around z axis. Exploiting this property we do a coordinate

transformation in the velocity space. This enables us to reduce the number of independent variables in the velocity space from three to two. Consider the Boltzmann equation for $f(x,y,z,u,v,w,t)$,

$$f_t + \mathbf{u}\nabla_{\mathbf{x}} f + \mathbf{F}\nabla_{\mathbf{u}} f = \int s(\mathbf{u}',\mathbf{u}) f(\mathbf{u}') d\mathbf{u}' - \int s(\mathbf{u},\mathbf{u}') f(\mathbf{u}) d\mathbf{u}'.$$

Then consider the polar transformation: (k,θ,ϕ) to (u,v,w) via $u = k\sin\theta\cos\phi$, $v = k\sin\theta\sin\phi$, and $w = k\cos\theta$. Then Boltzmann equation can be written as:

$$f_t + k\sin\theta\cos\phi f_x + k\sin\theta\sin\phi f_y + k\cos\theta f_z +$$

$$\{F_x\sin\theta\cos\phi + F_y\sin\theta\sin\phi + F_z\cos\theta\} f_k$$

$$\{F_x\frac{\cos\phi\cos\theta}{k} + F_y\frac{\sin\phi\cos\theta}{k} - F_z\frac{\sin\theta}{k}\} f_\theta$$

$$\{-F_x\frac{\sin\phi}{k\sin\theta} + F_y\frac{\cos\phi}{k\sin\theta}\} f_\phi =$$

$$\int s(k',\theta',\phi',k,\theta,\phi) f(k',\theta',\phi') k'^2 \sin\theta' dk' d\theta' d\phi' -$$

$$\int s(k,\theta,\phi,k',\theta',\phi') f(k,\theta,\phi) k'^2 \sin\theta' dk' d\theta' d\phi'.$$

Let us assume f is only dependent on z,k,θ,t . Also let us introduce a new variable $\mu = \cos\theta$. Then the right hand side can be written as:

$$f_t + k\mu f_z + F_z\{\mu f_k + \frac{1-\mu^2}{k} f_\mu\}.$$

For discretization purposes we prefer to write it as:

$$f_t + k\mu f_z + F_z\{\mu f_k + \frac{2\mu f}{k} + \frac{((1-\mu^2)f)_\mu}{k}\}.$$

The complete system is:

$$f_t + k\mu f_z + F_z\{\mu f_k + \frac{2\mu f}{k} + \frac{((1-\mu^2)f)_\mu}{k}\} =$$

$$2\pi \int s(k',\mu',k,\mu) f(k',\mu') k'^2 dk' d\mu' - 2\pi \int s(k,\mu,k',\mu') f(k,\mu) k'^2 dk' d\mu',$$

$$\phi_{zz} = \frac{e}{\epsilon}(n - N_D),$$

$$n = 2\pi \int\int f(k,\mu)k^2 dk d\mu, \text{ and } \quad F_z = \frac{e}{m}\phi_z$$

The system is completed with initial value and boundary conditions. For the initial conditions we use a Maxwellian distribution:

$$f(z,k,\mu,0) = (\frac{m}{2\pi k_B T_0})^{\frac{3}{2}} exp(-\frac{mk^2}{2k_B T_0}).$$

The computational domain is the box : $[0, z_{max}] \times [k_{min}, k_{max}] \times [-1,1]$. There is no need for boundary conditions at $f(z,k,1)$, $f(z,k,-1)$,$f(0,k,\mu)$ for $\mu < 0$, and $f(z_{max},k,\mu)$ for $\mu > 0$. In the k direction we use the following:

$$f(z,k_{max},\mu) = 0$$

$$f(z,k_{min},\mu) = f(z,k_{min},-\mu)$$

To motivate the last condition let us look at the characteristic lines in (k,μ) space. The characteristic lines are defined as integral curves of:

$$\frac{dk}{ds} = F_z\mu \qquad \frac{d\mu}{ds} = \frac{F_z(1-\mu^2)}{k}$$

In the (u,v,w) space they correspond to

$$\frac{du}{ds} = 0 \quad \frac{dv}{ds} = 0 \quad \frac{dw}{ds} = F_z$$

(See figure 1) To remove the singularity in (k,μ) space we remove a ball of radius k_{min} centered at the origin of (u,v,w). Once the ball is removed we identify the upper hemi-sphere with the lower hemi-sphere. Therefor point $(0,0,k_{min})$ is identified with point $(0,0,-k_{min})$, etc (see figure 2). This is equivalent to identifying (k,μ) with $(k,-\mu)$. Finally we need to specify the boundary conditions for the inflow and outflow of electrons.

$$f(0,k,\mu) \text{ if } \mu > 0 \qquad \text{and} \qquad f(z_{max},k,\mu) \text{ if } \mu < 0$$

Choosing the appropriate values is part of the physical modeling of the device under consideration. For this device we choose $\frac{\partial f}{\partial z} = 0$.

In our calculations we considered the following scattering terms [9]:

$$\int s(\mathbf{u}', \mathbf{u}) f(\mathbf{u}') d\mathbf{u}' - \int s(\mathbf{u}, \mathbf{u}') f(\mathbf{u}) d\mathbf{u}',$$

where,

$$s(\mathbf{u}, \mathbf{u}') = s_{ac}(\mathbf{u}, \mathbf{u}') + s_{op}^{em}(\mathbf{u}, \mathbf{u}') + s_{op}^{abs}(\mathbf{u}, \mathbf{u}'),$$

$$s_{ac}(\mathbf{u}, \mathbf{u}') = \frac{1}{(2\pi)^3}(\frac{m}{\hbar})^3 \frac{2\pi k_B T_0 E_{ac}^2}{\hbar u_l^2 \rho} \delta[E(\mathbf{u}') - E(\mathbf{u}))],$$

$$s_{op}^{em}(\mathbf{u}, \mathbf{u}') = \frac{1}{(2\pi)^3}(\frac{m}{\hbar})^3 \frac{\pi (D_t K)^2}{\rho \omega_{op}} N_{op}^{+} \delta[E(\mathbf{u}') - E(\mathbf{u}) + \hbar\omega_{op}],$$

$$s_{op}^{abs}(\mathbf{u}, \mathbf{u}') = \frac{1}{(2\pi)^3}(\frac{m}{\hbar})^3 \frac{\pi (D_t K)^2}{\rho \omega_{op}} N_{op} \delta[E(\mathbf{u}') - E(\mathbf{u}) - \hbar\omega_{op}],$$

where E is energy of an electron and is given by $E(\mathbf{u}^2) = \frac{1}{2} m \mathbf{u}^2 = \frac{1}{2} m k^2$.

The corresponding terms in the hydrodynamic model can be calculated by computing the following integral:

$$\int_0^{\infty} k^2 \int_{-1}^{1} f(k, \mu) d\mu \int_0^{2\pi} h(k, \mu, \phi) d\phi.$$

The quantities of interest are:

$$h(k, \mu, \phi) = 1, u, v, w, u^2, v^2, w^2, uv, vw, wu, uk^2, vk^2, wk^2,$$

$$< 1, f >= 2\pi \int_0^{+\infty} \int_{-1}^{1} k^2 f(k, \mu) dk d\mu,$$

$$< w, f >= 2\pi \int_0^{+\infty} \int_{-1}^{1} \mu k^3 f(k, \mu) dk d\mu,$$

$$< v, f >= 0,$$

$$< u, f >= 0,$$

$$< u^2, f >=< v^2, f >= \pi \int_0^{+\infty} \int_{-1}^{1} (1 - \mu^2) k^4 f(k, \mu) dk d\mu,$$

$$< w^2, f >= 2\pi \int_0^{+\infty} \int_{-1}^{1} \mu^2 k^4 f(k, \mu) dk d\mu,$$

$$< uv, f >= 0,$$

$$< uw, f >= 0,$$

$$< vw, f >= 0,$$

$$< uk^2, f >= 0,$$

$$< vk^2, f >= 0,$$

$$< wk^2, f >= 2\pi \int_0^{+\infty} \int_{-1}^{1} \mu k^5 f(k,\mu) dk d\mu.$$

The heat conduction term is:

$$\frac{1}{2} m(< wk^2, f > - \frac{< w, f >}{< 1, f >}\{3 < w^2, f > + < u^2, f > + < v^2, f >\} + 2\frac{< w, f >^3}{< 1, f >^2}).$$

Temperature is calculated via:

$$T_{11} = \frac{< u^2, f > - < u, f >^2}{< 1, f >},$$

$$T_{33} = \frac{< w^2, f > - < w, f >^2}{< 1, f >}.$$

4 The ballistic diode problem

As a model problem, we simulate the flow of electrons in a submicron $n^+ - n - n^+$ silicon diode. This device models the channel in a MOSFET. The diode begins with an n^+ "source" region, is followed by an n "channel" region, and ends with an n^+ "drain" region. The effects of holes may be neglected for the ballistic diode problem. For a discussion of the units and the proper constants we refer the reader to (Fatemi-Jerome-Osher) [3]. For the constants that are not in the above reference we use the following values:

$$N_{op} = (e^{\frac{\hbar\omega_{op}}{k_B T_0}} - 1)^{-1} \quad N_{op}^+ = N_{op} + 1$$

$$E_{ac} = 5.0 \text{ ev} \quad \hbar = 1.055 \times 10^{-34} \quad u_l = 9.0 \times 10^5 cm/sec$$
$$\rho = 2.33 gr/cm^3 \quad D_t K = 15.5 \times 10^8 ev/cm \quad \hbar\omega = 0.063 ev$$

5 Numerical Scheme

The numerical scheme used in these calculations uses explicit time stepping and upwind finite differences. The system can be abstractly represented by:

$$f_t = F(f, \phi) \quad \Delta\phi = G(f)$$

The second equation is linear and one dimensional. Its solution is rather trivial. One can solve for ϕ and substitute in the first equation.

$$f_t = F(f, \Delta^{-1}(G(f)))$$

This results in a nonlinear hyperbolic equation. Non-linearity comes from multiplication of $\nabla\phi$ by $\nabla_{\mathbf{u}} f$. This is the philosophy used in discretizing these equations.

Let a grid in (z, k, μ, t) space be defined by:

$$f^n_{sij} = f(s\Delta z, i\Delta k, , j\Delta\mu, n\Delta t) = f(z_s, k_i, \mu_j, t_n)$$

Then define backward differences as $D^-_z f_{sij} = \frac{(f_{sij} - f_{s-1i,j})}{\Delta z}$, forward differences as $D^+_z f_{sij} = \frac{(f_{s+1,ij} - f_{sij})}{\Delta z}$,and central differences as $D^0_z f_{sij} = \frac{(f_{s+1,ij} - f_{s-1,ij})}{2\Delta z}$. Then the numerical scheme is:

$$D^+_z D^-_z \phi^n_s = \frac{e}{\epsilon}(n_s - n_{Ds}), \quad F_s = \frac{e}{m} D^0_z \phi_s,$$

$$\frac{f^{n+1} - f^n}{\Delta t} + k\mu \frac{\hat{f}_{s+\frac{1}{2}} - \hat{f}_{s-\frac{1}{2}}}{\Delta z} + F_z\{\mu \frac{\hat{f}_{i+\frac{1}{2}} - \hat{f}_{i-\frac{1}{2}}}{\Delta k} + \frac{2\mu \bar{f}_i}{k} + \frac{\hat{g}_{j+\frac{1}{2}} - \hat{g}_{j-\frac{1}{2}}}{k\Delta\mu}\} = S_{sij},$$

$$\bar{f}_i = \frac{\hat{f}_{i+\frac{1}{2}} + \hat{f}_{i-\frac{1}{2}}}{2(1 + \frac{\Delta k^2}{4k^2})},$$

$$n_s = 2\pi \sum_j \sum_i (k_i^2 + \frac{\Delta k^2}{4}) f_{sij} \Delta k \Delta\mu.$$

The definitions for n_s and $\bar{f}$ are chosen such that in each time step mass is conserved . These definitions were motivated by the following argument. Note that:

$$k^2(f_k + \frac{2f}{k}) = (k^2 f)_k.$$

Then we discretize:

$$\Delta k k^2(f_k + \frac{2f}{k}) \approx (k^2 f)_{i+\frac{1}{2}} - (k^2 f)_{i-\frac{1}{2}}$$
$$= (k^2_{i+\frac{1}{2}} - k^2_{i-\frac{1}{2}}) f_{i+\frac{1}{2}} + k^2_{i-\frac{1}{2}}(f_{i+\frac{1}{2}} - f_{i-\frac{1}{2}})$$
$$= (k^2_{i+\frac{1}{2}} - k^2_{i-\frac{1}{2}}) f_{i-\frac{1}{2}} + k^2_{i+\frac{1}{2}}(f_{i+\frac{1}{2}} - f_{i-\frac{1}{2}}).$$

Therefore:

$$k^2(f_k + \frac{2f}{k}) \approx \frac{1}{2}(k^2_{i+\frac{1}{2}} + k^2_{i-\frac{1}{2}})\{\frac{f_{i+\frac{1}{2}} - f_{i-\frac{1}{2}}}{\Delta k} + \frac{2(k^2_{i+\frac{1}{2}} - k^2_{i-\frac{1}{2}})}{(k^2_{i+\frac{1}{2}} + k^2_{i-\frac{1}{2}})} \frac{f_{i+\frac{1}{2}} + f_{i-\frac{1}{2}}}{2}\}$$
$$= (k_i^2 + \frac{\Delta k^2}{4})\{\frac{f_{i+\frac{1}{2}} - f_{i-\frac{1}{2}}}{\Delta k} + \frac{2}{k_i} \frac{(f_{i+\frac{1}{2}} + f_{i-\frac{1}{2}})}{2(1 + \frac{\Delta k^2}{4k_i^2})}\}.$$

Flux functions, $\hat{f}_{s+\frac{1}{2}}, \hat{f}_{i+\frac{1}{2}}$, and$\hat{g}_{j+\frac{1}{2}}$ are defined in the following fashion:

$$\hat{f}_{s+\frac{1}{2}} = f_s \text{ if } k\mu > 0, \qquad \hat{f}_{s+\frac{1}{2}} = f_{s+1} \text{ if } k\mu < 0,$$

$$\hat{f}_{i+\frac{1}{2}} = f_i \text{ if } F_z\mu > 0, \qquad \hat{f}_{i+\frac{1}{2}} = f_{i+1} \text{ if } F_z\mu < 0,$$

$$\hat{g}_{j+\frac{1}{2}} = (1-\mu^2) f_j \text{ if } F_z > 0, \qquad \hat{g}_{j+\frac{1}{2}} = (1-\mu^2) f_{j+1} \text{ if } F_z < 0.$$

The scattering terms S_{sij} were calculated using trapezoidal rule. The scattering term, s_{ac}, was analytically integrated in the k space. For integrating s_{op}^{em} and s_{op}^{abs} an approximation to the δ function was used. The particular approximation was $\delta(x) = \frac{.75}{\epsilon}(1 - \frac{x^2}{\epsilon^2})$. Trapezoidal rule was used as the integration formula for calculating the moments.

One of the major results of the upwind differencing is that the truncation error contains a second order operator with the right constant in front of it. This introduces the so called "artificial viscosity" in the method. Its effect is to smear out sharp gradients in the solution. This can be remedied by refining the mesh at those regions. An alternative solution is to use higher order methods for calculating the fluxes. In the calculations done for the Hydrodynamic model [3] use of a sixth order stencil minimized the diffusion. For BTE calculations we had to refine the mesh in areas where n_D has high gradient. It can be easily seen that the truncation error of this discretization is:

$$\frac{\Delta t}{2} f_{tt} - \frac{k|\mu|\Delta z}{2} f_{zz} - \frac{|F_z\mu|\Delta k}{2} f_{kk} - \frac{|F_z\mu|\Delta k}{k(1 + \frac{\Delta k^2}{4k^2})} f_k$$

$$+\frac{|F_z|\Delta\mu}{k}f+\frac{2|F_z|\mu\Delta\mu}{k}f_\mu-\frac{|F_z|(1-\mu^2)\Delta\mu}{2k}f_{\mu\mu}.$$

Since this is an explicit time stepping the time steps have to be limited to satisfy the Courant-Friedrichs-Lewy condition. Necessary CFL conditions for stability are:

$$\frac{k|\mu|\Delta t}{\Delta z}<1,\qquad \frac{|F_z\mu|\Delta t}{\Delta k}<1,\qquad \text{and}\quad \frac{|F_z|(1-\mu^2)\Delta t}{k\Delta\mu}<1.$$

In practice this translates into:

$$\Delta t<\frac{\Delta z}{k_{max}},\quad \Delta t<\frac{\Delta k}{Max|F_z|},\quad \text{and}\quad \Delta t<\frac{k_{min}\Delta\mu}{Max|F_z|}.$$

In computations an automatic time step was chosen based on the above criteria and no instability was observed.

6 Numerical Results

For comparison we chose the n^+nn^+ structure. In figure three we show the calculated velocity. Note that the spike is missing in the Boltzmann solution. In figure four for reference we compare the Mach numbers. Note that the flow is subsonic. Also the velocity from BTE code is higher, possibly because the scattering constants are low and/or we need to consider more scattering mechanisms. In figure five we compare the calculated temperatures from the Hydrodynamic model and the BTE code. As can be seen T_{33} is a little higher than $T_{11}=T_{22}$. The difference can be approximated by viscosity terms and it turns out that these terms are small and can be neglected. In figure six we compare the viscosity terms. The solid curve is $n\frac{2T_{33}-T_{22}-T_{11}}{3}$ and the doted line is $-\frac{4}{3}\tau_p nTw_z$. Calculations were done with viscosity terms included in the Hydro model and they had small effect on the velocity profile. This could be expected since the Reynolds number of the flow is around 10^3. In figure seven the solid line shows the heat conduction term from BTE and the doted line shows the heat conduction term calculated from Fourier law, κnT_z. Where for κ we use the Wiedmann-Franz law [1]. As can be seen the approximation is reasonable except in the drain.

In the next figure we plot the τ_p as calculated from the BTE, the model suggested by Baccarni and Wordeman [1] , and the model suggested by S. Lee [11]. The unusual dips in the solid line at $z = .3$ and $z = .7$ are from numerical inaccuracies. But as can be seen the model for τ_p is not accurate. Two features are certain. The dependence of τ on $\frac{1}{T}$ is too strong. The other feature is that as electrons enter the channel the relaxation of the high velocity electrons requires certain distant. This distant seems to be shorter for relaxation of the second moment (Temperature) but longer for first moment of the scattering term and third moment of the density (Heat Conduction term). Finally in figure nine we show the density distribution as a function of velocity at different points in the device. The density is integrated over all anglesμ. The density is close to gaussian at $x = 0.$ and $x = 1.0$ but deviates substantially from gaussian in the channel.

7 Conclusion

We presented a simple scheme for solving the Boltzmann equation coupled to Poisson in one dimension. The computer time was modest for one dimensional case. For extension to two or three dimension a more efficient algorithm is needed. The results from the BTE calculations were integrated over velocity space to obtain measurable physical quantities. The results were compared with the results from the Hydrodynamic model. It turned out that the models for heat conduction and viscosity were adequate. Viscosity has small effect on the flow and can be neglected. The model for τ_p is not accurate and seems to be source of the spurious oscillations in the velocity profiles calculated from the Hydrodynamic model.

References

[1] G. Baccarani and M. R. Wordeman, An investigation of steady-state velocity overshoot effects in Si and GaAs devices, *Solid State Electronics*, vol.**28**, pp. 407–416, (1985).

[2] K. Bløtekjær, Transport equations for electrons in two-valley semiconductors, *IEEE Transactions on Electron Devices*, vol. **ED-17**, pp. 38–47, (1970).

[3] E. A. Fatemi, J. W. Jerome, and S. Osher, Solution of the hydrodynamic device model using high-order non-oscillatory shock capturing algorithms, *IEEE Transactions on Computer-Aided Design of Integrated Circuits and Systems*, vol. **10**, no. 2, (1991).

[4] E. Fatemi, C. Gardner, J. Jerome, S. Osher, and D. Rose, Simulation of a steady-state electron shock wave in a submicron semiconductor device using high-order upwind methods, *Computational Electronics*, Hess, Leburton, and Ravioli, eds.,(Kluwer Academic Publishers. 1991).

[5] G. I. Gamba, Stationary transonic solutions of a one-dimensional hydrodynamic model for semiconductors, Technical Report #143, Center for Applied Mathematics, Purdue University.

[6] C. L. Gardner, J. W. Jerome, and D. J. Rose, Numerical methods for the hydrodynamic device model: Subsonic flow, *IEEE Transactions on Computer-Aided Design of Integrated Circuits and Systems*, vol.**8**, pp. 501–507, (1989).

[7] H. L. Grubin and J. P. Kreskovsky, The role of boundary conditions in near and submicrometer length gallium arsenide structures, *VLSI Electronics:Microstructure Science Vol. 10,* , N. G. Einspruch and R. S. Bauer, Eds.,(Academic Press, New York, 1985), pp. 237-321.

[8] K. Huang, *Statistical Mechanics*, (John Wiley & Sons, New York, 1987).

[9] C. Jacoboni and L. Reggiani, The monte carlo method for the solution of charge transport in semiconductors with applications to covalent Materials, *Rev. Mod. Phys.*, vol. **55**, no. 3, (1983).

[10] H. B. Keller and B. Wendroff, On the formulation and analysis of numerical methods for time dependent transport equations, *Communications on Pure and Applied Mathematics*, vol.**X**, pp. 567-582, (1957).

[11] S. Lee, Ph. D. thesis, University of Massachusetts, (1990).

[12] B. Niclot, P. Degond, and F. Poupaud, Deterministic particle simulations of the boltzmann transport equation of semiconductors, *Journal of Computational Physics* , **78**, pp. 313-349 (1988).

[13] F. Odeh, M. Rudan, and J. White, Numerical solution of the hydrodynamic model for a one-dimensional semiconductor device, COMPEL, vol. **5**, pp. 149-183, (1986).

[14] C. W. Shu and S. Osher, Efficient implementation of essentially non-oscillatory shock capturing schemes, II, *J. Comp. Phys.*, vol. **83**, pp. 32-78, (1989).

Figure Captions

Figure 1. Characteristic Curves in Velocity Space

Figure 2. Boundary Conditions for k_{min}.

Figure 3. Electron Velocity

Figure 4. Mach Number of the Flow

Figure 5. Temperature (Hydro), T_{11}, and T_{33}

Figure 6. Viscosity Comparison

Figure 7. Heat Conduction Comparison

Figure 8. Momentum Relaxation Time Comparison

Figure 9. Density Distribution Comparison

Figure 1. Characteristic Curves in Velocity Space

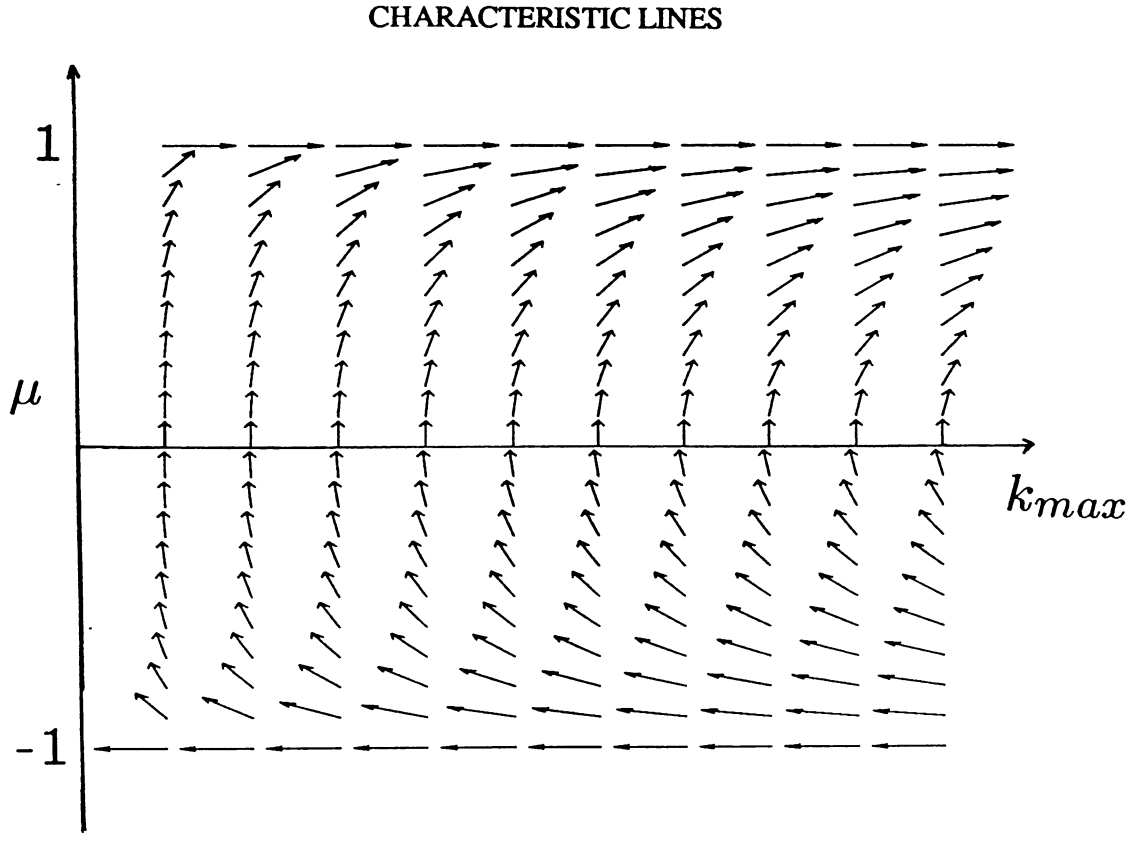

Figure 2. Boundary Conditions for k_{min}.

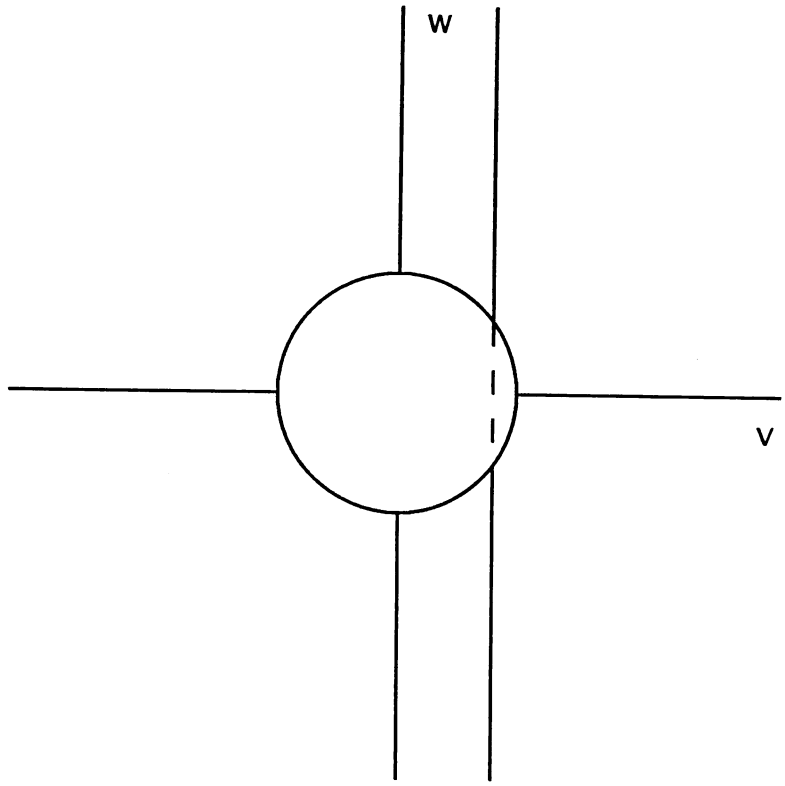

Figure 3. Electron Velocity

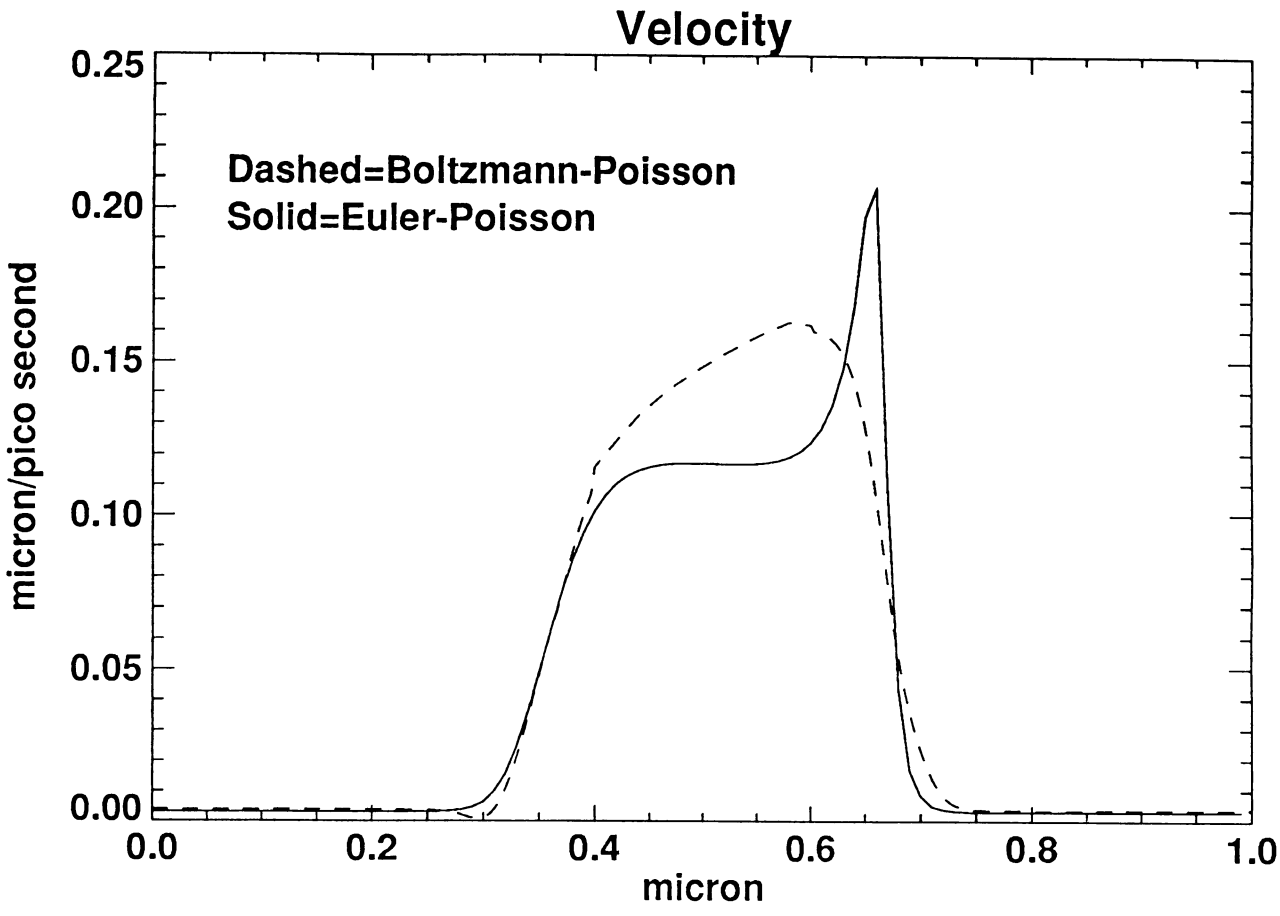

Figure 4. Mach Number of the Flow

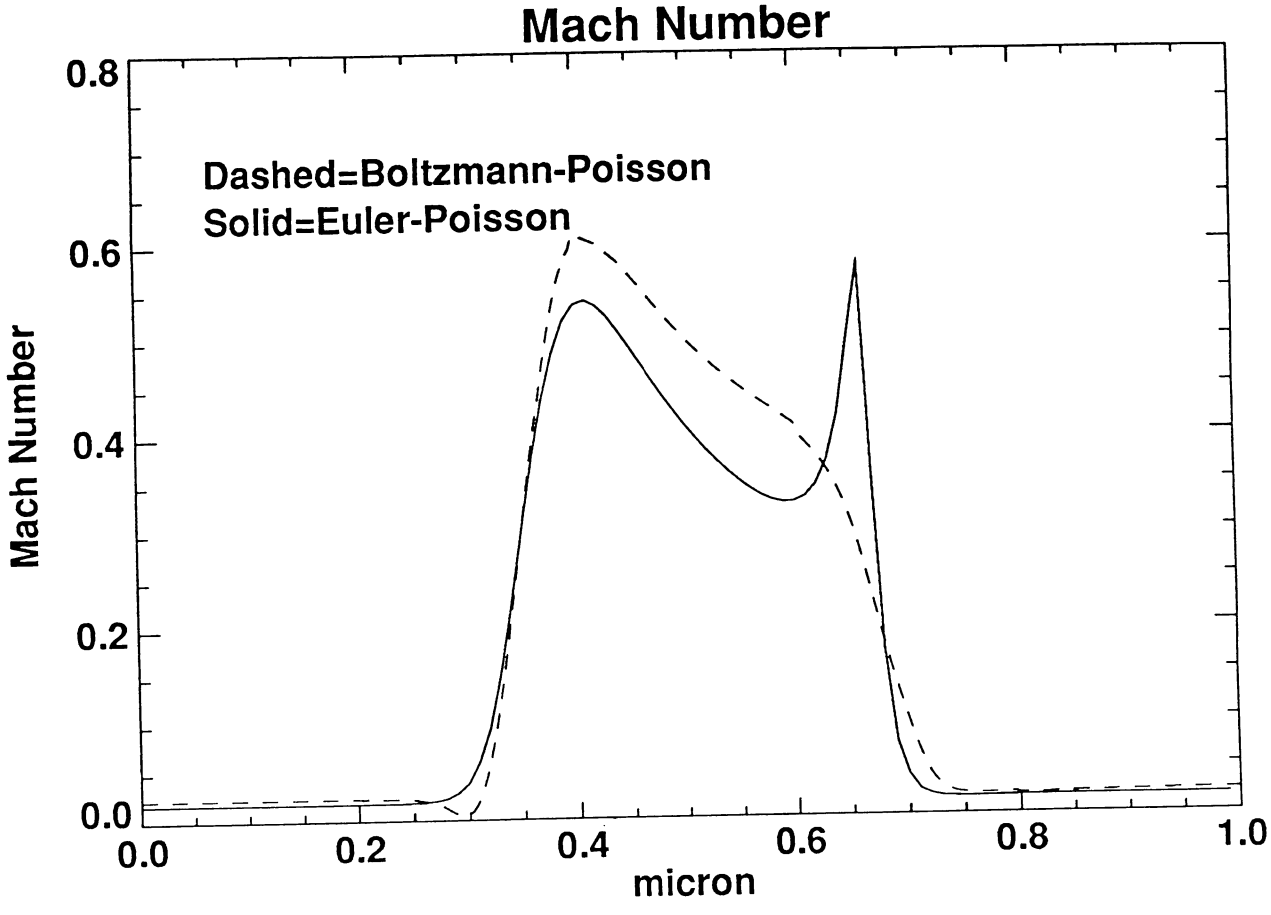

Figure 5. Temperature (Hydro), T_{11}, and T_{33}

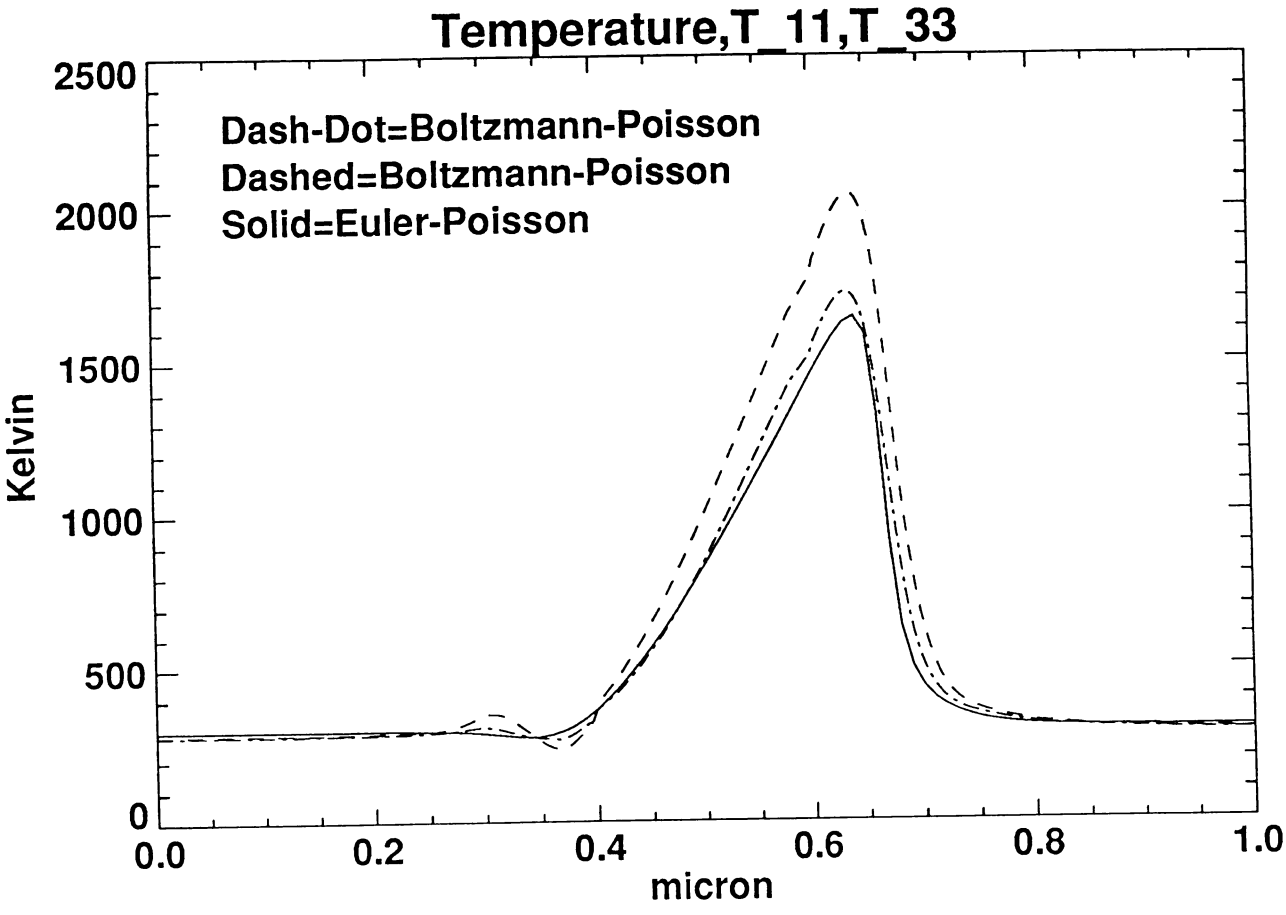

Figure 6. Viscosity Comparison

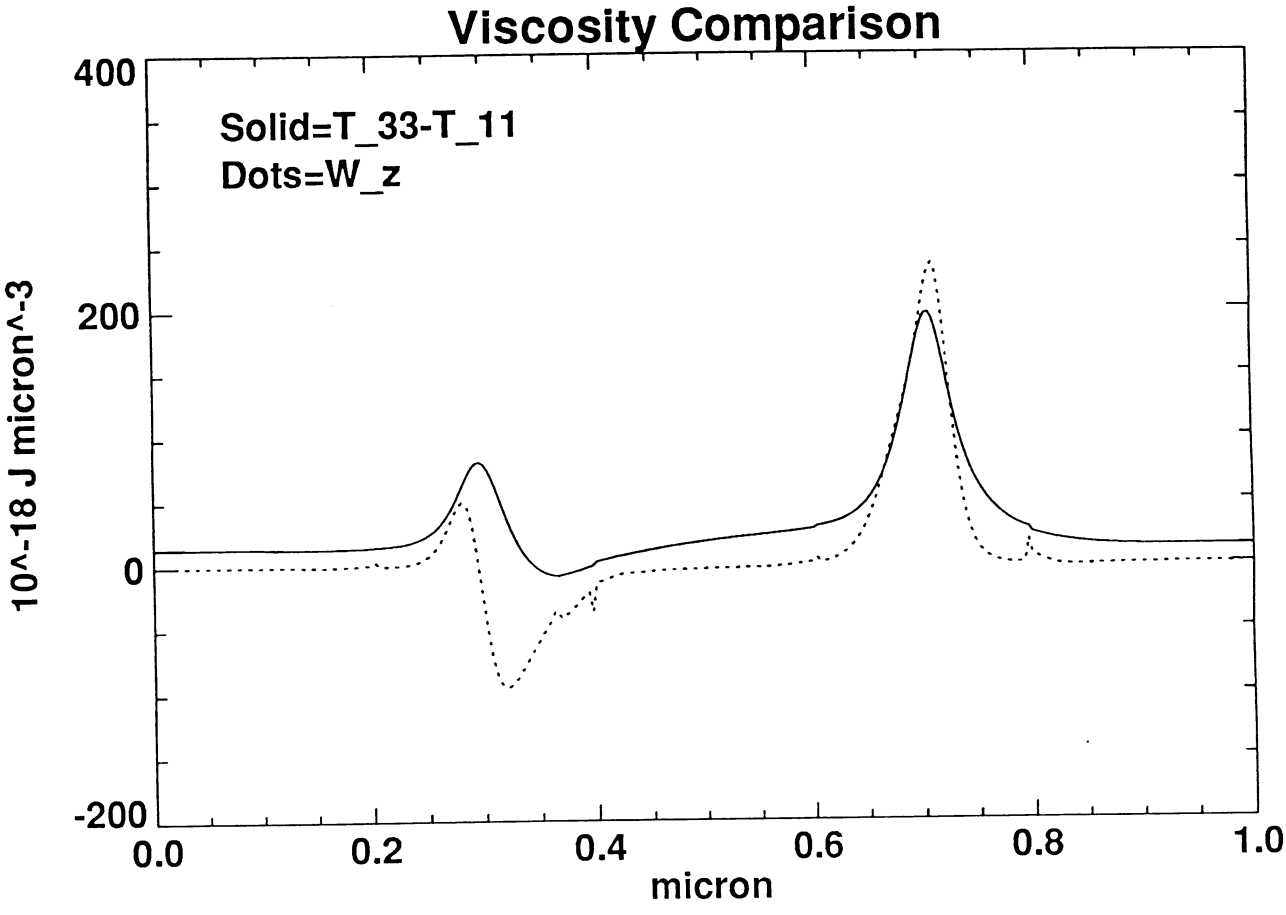

Figure 7. Heat Conduction Comparison

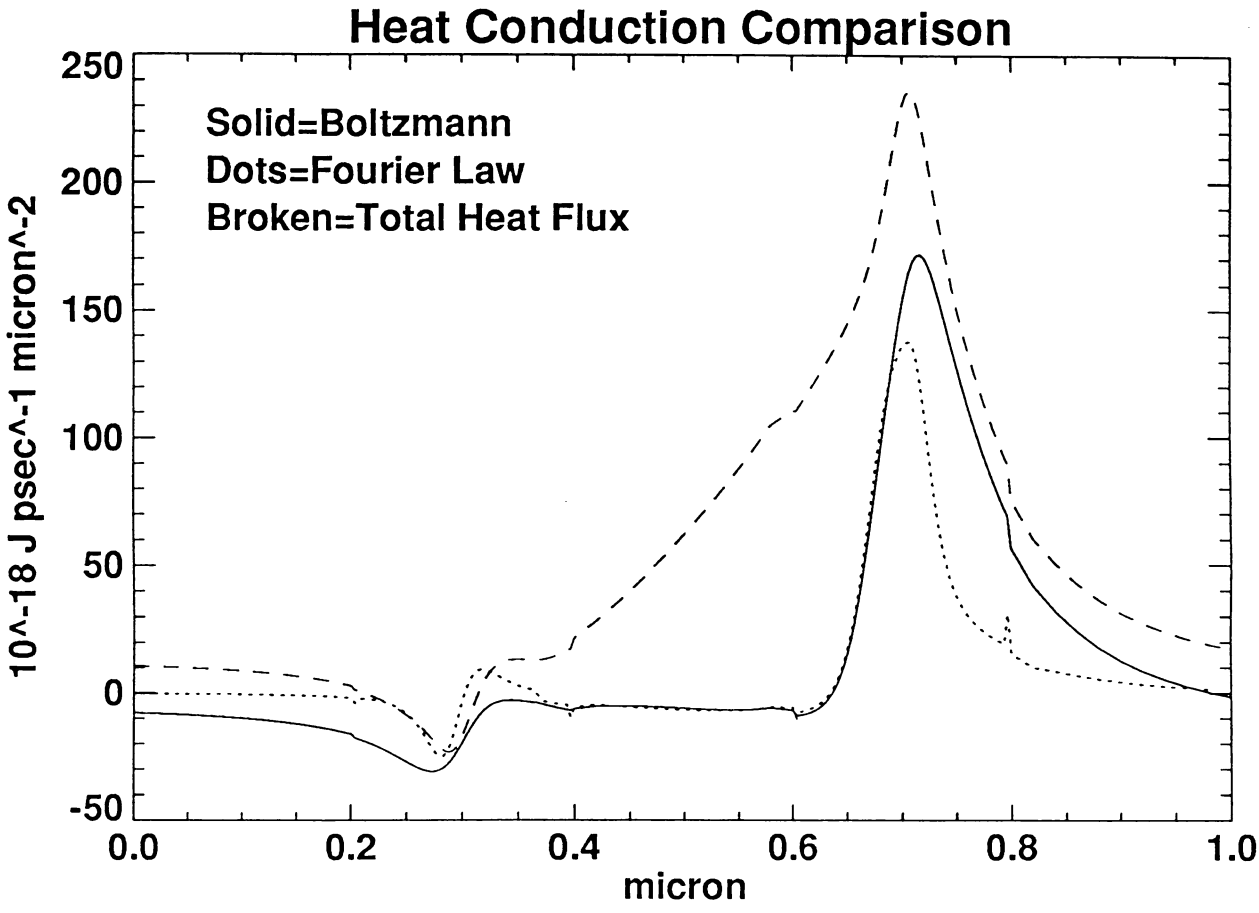

Figure 8. Momentum Relaxation Time Comparison

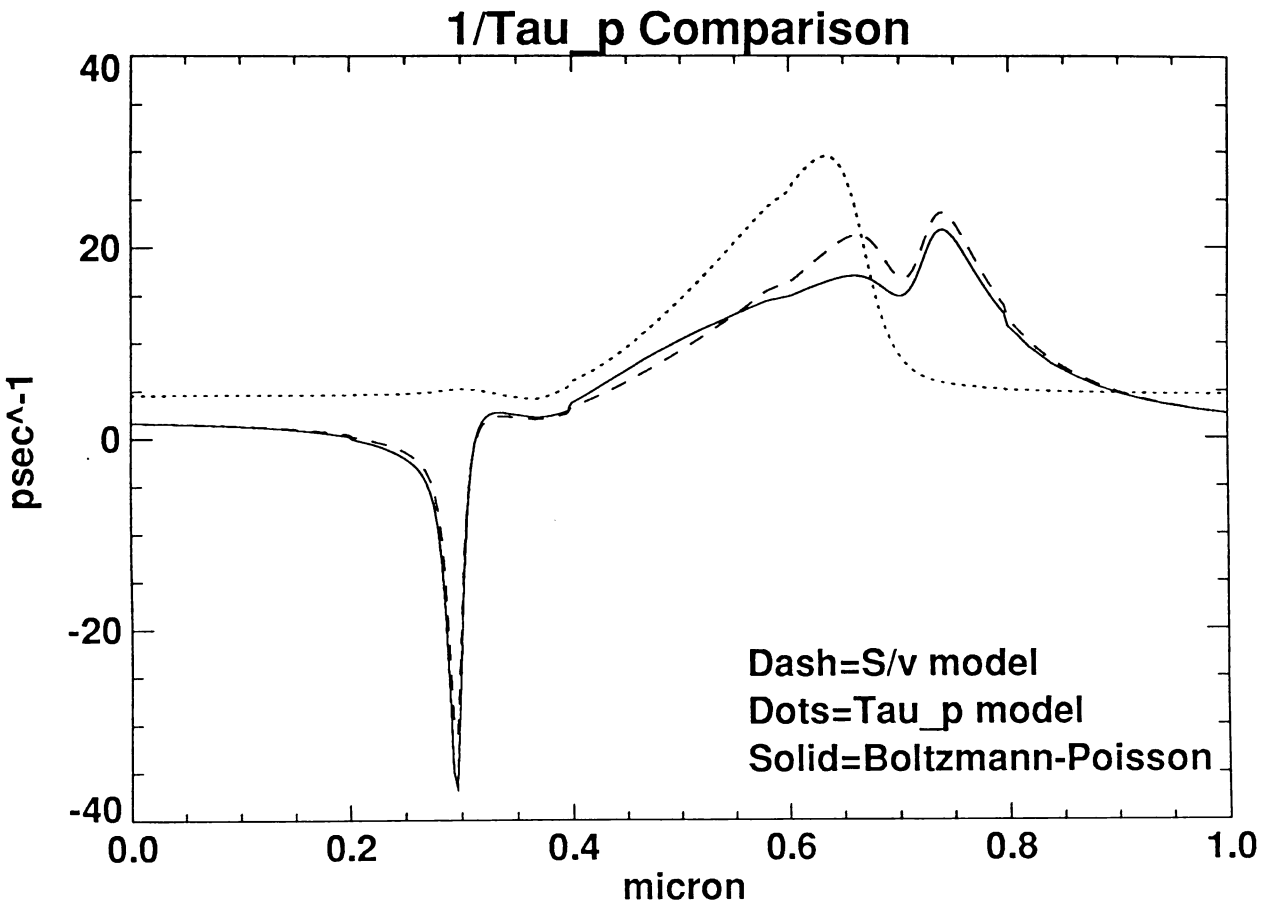

Figure 9. Density Distribution Comparison

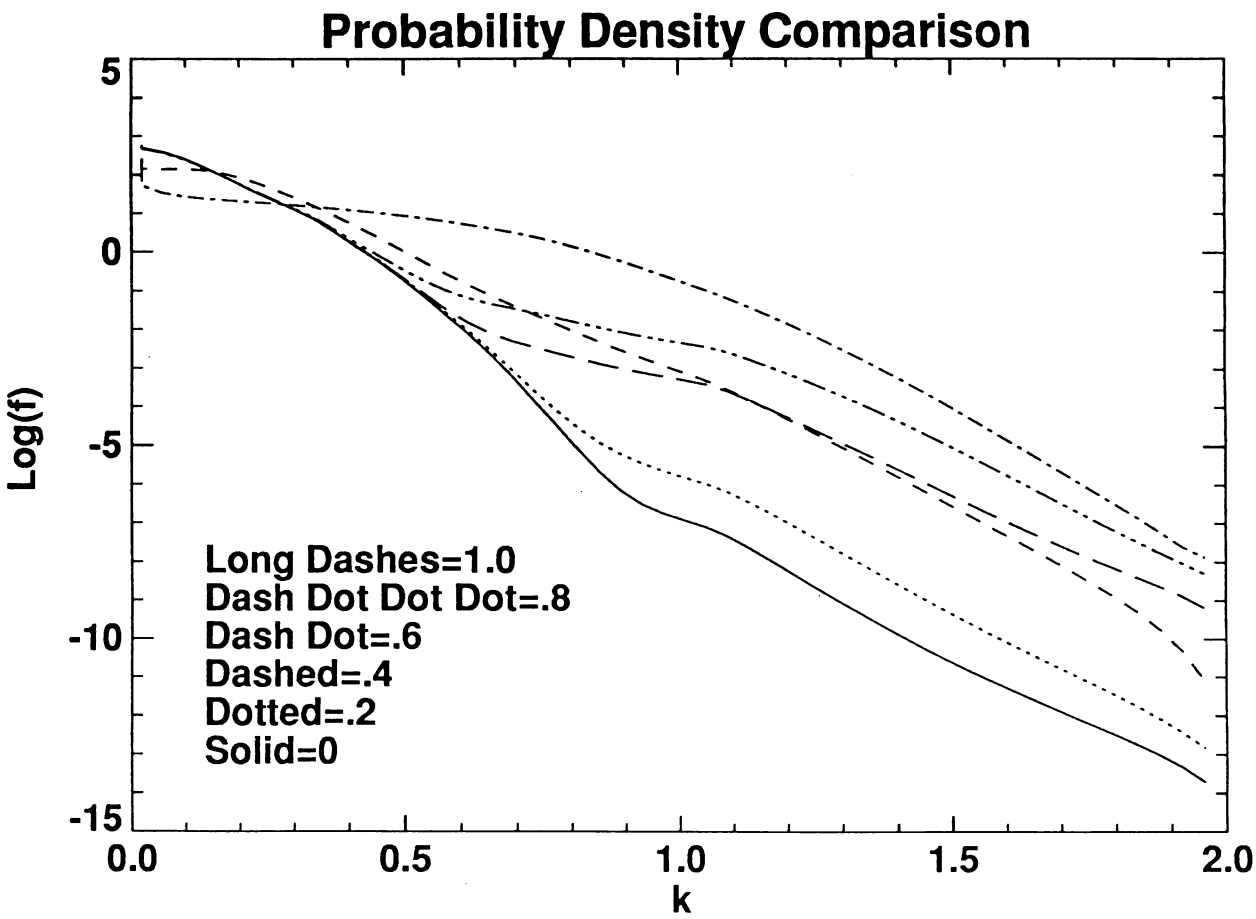

Recent IMA Preprints

#	Author/s	Title
892	**E.G. Kalnins, Willard Miller, Jr. and Sanchita Mukherjee**	Models of q-algebra representations: the group of plane motions
893	**T.R. Hoffend Jr. and R.K. Kaul**	Relativistic theory of superpotentials for a nonhomogeneous, spatially isotropic medium
894	**Reinhold von Schwerin**	Two metal deposition on a microdisk electrode
895	**Vladimir I. Oliker and Nina N. Uraltseva**	Evolution of nonparametric surfaces with speed depending on curvature, III. Some remarks on mean curvature and anisotropic flows
896	**Wayne Barrett, Charles R. Johnson, Raphael Loewy and Tamir Shalom**	Rank incrementation via diagonal perturbations
898	**Mingxiang Chen, Xu-Yan Chen and Jack K. Hale**	Structural stability for time-periodic one-dimensional parabolic equations
899	**Hong-Ming Yin**	Global solutions of Maxwell's equations in an electromagnetic field with the temperature-dependent electrical conductivity
900	**Robert Grone, Russell Merris and William Watkins**	Laplacian unimodular equivalence of graphs
901	**Miroslav Fiedler**	Structure-ranks of matrices
902	**Miroslav Fiedler**	An estimate for the nonstochastic eigenvalues of doubly stochastic matrices
903	**Miroslav Fiedler**	Remarks on eigenvalues of Hankel matrices
904	**Charles R. Johnson, D.D. Olesky, Michael Tsatsomeros and P. van den Driessche**	Spectra with positive elementary symmetric functions
905	**Pierre-Alain Gremaud**	Thermal contraction as a free boundary problem
906	**K.L. Cooke, Janos Turi and Gregg Turner**	Stabilization of hybrid systems in the presence of feedback delays
907	**Robert P. Gilbert and Yongzhi Xu**	A numerical transmutation approach for underwater sound propagation
908	**LeRoy B. Beasley, Richard A. Brualdi and Bryan L. Shader**	Combinatorial orthogonality
909	**Richard A. Brualdi and Bryan L. Shader**	Strong hall matrices
910	**Håkan Wennerström and David M. Anderson**	Difference versus Gaussian curvature energies; monolayer versus bilayer curvature energies applications to vesicle stability
911	**Shmuel Friedland**	Eigenvalues of almost skew symmetric matrices and tournament matrices
912	**Avner Friedman, Bei Hu and J.L. Velazquez**	A Free Boundary Problem Modeling Loop Dislocations in Crystals
913	**Ezio Venturino**	The Influence of Diseases on Lotka-Volterra Systems
914	**Steve Kirkland and Bryan L. Shader**	On Multipartite Tournament Matrices with Constant Team Size
915	**Richard A. Brualdi and Jennifer J.Q. Massey**	More on Structure-Ranks of Matrices
916	**Douglas B. Meade**	Qualitative Analysis of an Epidemic Model with Directed Dispersion
917	**Kazuo Murota**	Mixed Matrices Irreducibility and Decomposition
918	**Richard A. Brualdi and Jennifer J.Q. Massey**	Some Applications of Elementary Linear Algebra in Combinations
919	**Carl D. Meyer**	Sensitivity of Markov Chains
920	**Hong-Ming Yin**	Weak and Classical Solutions of Some Nonlinear Volterra Integrodifferential Equations
921	**B. Leinkuhler and A. Ruehli**	Exploiting Symmetry and Regularity in Waveform Relaxation Convergence Estimation
922	**Xinfu Chen and Charles M. Elliott**	Asymptotics for a Parabolic Double Obstacle Problem
923	**Yongzhi Xu and Yi Yan**	An Approximate Boundary Integral Method for Acoustic Scattering in Shallow Oceans
924	**Yongzhi Xu and Yi Yan**	Source Localization Processing in Perturbed Waveguides
925	**Kenneth L. Cooke and Janos Turi**	Stability, Instability in Delay Equations Modeling Human Respiration
926	**F. Bethuel, H. Brezis, B.D. Coleman and F. Hélein**	Bifurcation Analysis of Minimizing Harmonic Maps Describing the Equilibrium of Nematic Phases Between Cylinders
927	**Frank W. Elliott, Jr.**	Signed Random Measures: Stochastic Order and Kolmogorov Consistency Conditions
928	**D.A. Gregory, S.J. Kirkland and B.L. Shader**	Pick's Inequality and Tournaments
929	**J.W. Demmel, N.J. Higham and R.S. Schreiber**	Block LU Factorization
930	**Victor A. Galaktionov and Juan L. Vazquez**	Regional Blow-Up in a Semilinear Heat Equation with Convergence to a Hamilton-Jacobi Equation
931	**Bryan L. Shader**	Convertible, Nearly Decomposable and Nearly Reducible Matrices
932	**Dianne P. O'Leary**	Iterative Methods for Finding the Stationary Vector for Markov Chains
933	**Nicholas J. Higham**	Perturbation theory and backward error for $AX - XB = C$
934	**Z. Strakos and A. Greenbaum**	Open questions in the convergence analysis of the lanczos process for the real symmetric eigenvalue problem
935	**Zhaojun Bai**	Error analysis of the lanczos algorithm for the nonsymmetric eigenvalue problem
936	**Pierre-Alain Gremaud**	On an elliptic-parabolic problem related to phase transitions in shape memory alloys
937	**Bojan Mohar and Neil Robertson**	Disjoint essential circuits in toroidal maps

939 **Bojan Mohar and Svatopluk Poljak** Eigenvalues in combinatorial optimization
940 **Richard A. Brualdi, Keith L. Chavey and Bryan L. Shader**, Conditional sign-solvability
941 **Roger Fosdick and Ying Zhang**, The torsion problem for a nonconvex stored energy function
942 **René Ferland and Gaston Giroux**, An unbounded mean-field intensity model: Propagation of the convergence of the empirical laws and compactness of the fluctuations
943 **Wei-Ming Ni and Izumi Takagi**, Spike-layers in semilinear elliptic singular Perturbation Problems
944 **Henk A. Van der Vorst and Gerard G.L. Sleijpen**, The effect of incomplete decomposition preconditioning on the convergence of conjugate gradients
945 **S.P. Hastings and L.A. Peletier**, On the decay of turbulent bursts
946 **Apostolos Hadjidimos and Robert J. Plemmons**, Analysis of p-cyclic iterations for Markov chains
947 **ÅBjörck, H. Park and L. Eldén**, Accurate downdating of least squares solutions
948 **E.G. Kalnins, Willard Miller, Jr. and G.C. Williams**, Recent advances in the use of separation of variables methods in general relativity
949 **G.W. Stewart**, On the perturbation of LU, Cholesky and QR factorizations
950 **G.W. Stewart**, Gaussian elimination, perturbation theory and Markov chains
951 **G.W. Stewart**, On a new way of solving the linear equations that arise in the method of least squares
952 **G.W. Stewart**, On the early history of the singular value decomposition
953 **G.W. STewart**, On the perturbation of Markov chains with nearly transient states
954 **Umberto Mosco**, Composite media and asymptotic dirichlet forms
955 **Walter F. Mascarenhas**, The structure of the eigenvectors of sparse matrices
956 **Walter F. Mascarenhas**, A note on Jacobi being more accurate than QR
957 **Raymond H. Chan, James G. Nagy and Robert J. Plemmons**, FFT-based preconditioners for Toeplitz-Block least squares problems
958 **Zhaojun Bai**, The CSD, GSVD, their applications and computations
959 **D.A. Gregory, S.J. Kirkland and N.J. Pullman**, A bound on the exponent of a primitive matrix using Boolean rank
960 **Richard A. Brualdi, Shmuel Friedland and Alex Pothen**, Sparse bases, elementary vectors and nonzero minors of compound matrices
961 **J.W. Demmel**, Open problems in numerical linear algebra
962 **James W. Demmel and William Gragg**, On computing accurate singular values and eigenvalues of acyclic matrices
963 **James W. Demmel**, The inherent inaccuracy of implicit tridiagonal QR
964 **J.J.L. Velázquez**, Estimates on the $(N-1)$-dimensional Hausdorff measure of the blow-up set for a semilinear heat equation
965 **David C. Dobson**, Optimal design of periodic antireflective structures for the Helmholtz equation
966 **C.J. van Duijn and Joseph D. Fehribach**, Analysis of planar model for the molten carbonate fuel cell
967 **Yongzhi Xu, T. Craig Poling and Trent Brundage**, Source localization in a waveguide with unknown large inclusions
968 **J.J.L. Velázquez**, Higher dimensional blow up for semilinear parabolic equations
969 **E.G. Kalnins and Willard Miller, Jr.**, Separable coordinates, integrability and the Niven equations
970 **John M. Chadam and Hong-Ming Yin**, A diffusion equation with localized chemical reactions
971 **A. Greenbaum and L. Gurvits**, Max-min properties of matrix factor norms
972 **Bei Hu**, A free boundary problem arising in smoulder combustion
973 **C.M. Elliott and A.M. Stuart**, The global dynamics of discrete semilinear parabolic equations
974 **Avner Friedman and Jianhua Zhang**, Swelling of a rubber ball in the presence of good solvent
975 **Avner Friedman and Juan J.L. Velázquez**, A time-dependence free boundary problem modeling the visual image in electrophotography
976 **Richard A. Brualdi, Hyung Chan Jung and William T. Trotter, Jr.**, On the poset of all posets on n elements
977 **Ricardo D. Fierro and James R. Bunch**, Multicollinearity and total least squares
978 **Adam W. Bojanczyk, James G. Nagy and Robert J. Plemmons**, Row householder transformations for rank-k Cholesky inverse modifications
979 **Chaocheng Huang**, An age-dependent population model with nonlinear diffusion in R^n
980 **Emad Fatemi and Faroukh Odeh**, Upwind finite difference solution of Boltzmann equation applied to electron transport in semiconductor devices
981 **Esmond G. Ng and Barry W. Peyton**, A tight and explicit representation of Q in sparse QR factorization
982 **Robert J. Plemmons**, A proposal for FFT-based fast recursive least-squares
983 **Anne Greenbaum and Zdenek Strakos**, Matrices that generate the same Krylov residual spaces
984 **Alan Edelman and G.W. Stewart**, Scaling for orthogonality
985 **G.W. Stewart**, Note on a generalized sylvester equation
986 **G.W. Stewart**, Updating URV decompositions in parallel